on silica gel (12 g, eluent = hexane–ethyl acetate, 12:1). The desired product was obtained as a mixture of two compounds by VPC analysis in the yields and ratios given in Table IV. A few fractions of the chromatographed material contained sufficiently pure material (ca. 97% by VPC) to allow spectral analysis of each compound. Minor isomer (**5b**): IR (film) 2950, 1750, 1725, 1050 cm^{-1}; 200 MHz NMR ($CDCl_3$) δ 0.86 (d, 3 H), 1.12 (m, 1 H), 1.58 (m, 4 H), 1.98 (bd, 1 H), 2.24 (s, 3 H), 2.42 (m, 1 H), 2.8–3.1 (m, 2 H), 3.65 (s, 3 H); low resolution mass spectrum for $C_{11}H_{18}O_3$ requires m/e 198, found m/e 198. Major isomer (**5a**): IR (film) 2930, 1740, 1720, 1370 cm^{-1}; 200 MHz NMR ($CDCl_3$) δ 0.92 (d, 3 H), 1.0–2.0 (m, 7 H), 2.14 (s, 3 H), 2.21 (t, 1 H), 2.78 (ddd, 1 H (J = 3.4, 11.0, 11.7 Hz)), 3.66 (s, 3 H); low resolution mass spectrum for $C_{11}H_{18}O_3$ requires m/e 198, found m/e 198.

(b) Using Benzophenone for Initiation. The reaction was carried out at 4 °C as in the previous experiment except that 0.10 mmol of benzophenone was used in place of perester 1. After the standard workup, VPC analysis gave the results listed in Table V.

(c) Using Benzoyl Peroxide for Initiation. To 1.0 mL benzene was added 1.0 mmol of **2**, 10.0 mmol of acetaldehyde, and 0.10 mmol benzoyl peroxide. After degassing with several freeze/pump/thaw cycles, the reaction tube was sealed under an Ar atmosphere and placed in an oil bath at 95 °C for 16 h. After the standard workup, VPC analysis gave the results listed in Table V.

Attempted Epimerization of Methyl 2-Acetyl-6-methylcyclohexanecarboxylate (5a and 5b). (a) Basic Conditions. The product mixture of **5a** and **5b** (100 mg, 0.5 mmol) obtained from initiation with perester (1) was dissolved in either benzene (2 mL) or CH_2Cl_2 (2 mL). One equivalent of DBU was added and each solution was refluxed for 24 h. VPC analysis of either reaction mixture indicated no change in the ratio of **5a** to **5b**.

(b) Acidic Conditions. The product mixture of **5a** and **5b** (100 mg, 0.5 mmol) obtained from initiation with perester 1 was dissolved in CH_2Cl_2 (2 mL) followed by addition of 0.1 equiv of *p*-TSA. The reaction was stirred at room temperature and monitored by VPC. After 24 h no change in the product ratio had occurred. Use of two drops of 5% HCl under the same conditions gave the same result.

Acknowledgment. This work was supported by the National Science Foundation (DMR No. 8404001). We are grateful for this support.

Evidence for an Unusual Charge-Transfer Complex in (Nitrophenacyl)anilines

Riaz F. Abdulla,* Donald B. Boyd,[1] Noel D. Jones,[1] and John K. Swartzendruber[1]

Lilly Research Laboratories, Eli Lilly and Company, Greenfield, Indiana 46140

Received February 5, 1985

The color of (nitrophenacyl)anilines can be explained from an X-ray crystallographic study that indicates that one such compound is planar and stacked in the crystal in an alternating "head-to-tail" arrangement. This arrangement permits an unusual charge transfer between two molecules of the same compound, with the aniline end being the donor and the nitrophenacyl end being the acceptor. The possibility of charge transfer is supported by MNDO, MINDO/3, and extended Hückel molecular orbital calculations.

The (nitrophenacyl)anilines have been known for many years. Over 100 years ago, Möhlau[2] noted that these compounds formed deeply colored crystals. However, the origin of their color has not been explained. We[3-7] and others[8,9] have observed that, depending on the substituents on the *N*-aryl group and on the phenacyl ring of **1**, com-

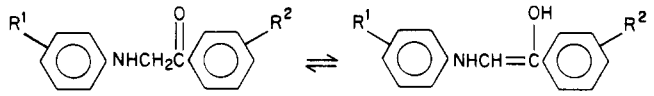

1 **2**

pounds show transmitted and reflected crystal color ranging from scarlet to orange to yellow. The compounds that are the most intensely colored are those which have electron sources on the aniline ring and are concomitantly substituted with strong electron sinks on the phenacyl nucleus (Table I).

Table I. Effect of Ring Substituents on the Color of the Phenacylanilines

1	R^1	R^2	color
a	H	4′-NO_2	scarlet[a]
b	4-CH_3O	3′-NO_2	orange[b]
c	2-CH_3	4′-NO_2	orange-red[a]
d	4-CH_3CO	4′-NO_2	yellow[a,c]
e	4-C_2H_5OCO	4′-NO_2	yellow[b,c]

[a] Reference 3. [b] Reference 4. [c] Reference 9.

Though the reactions of the phenacylanilines and those of the phenacyl chloroacetanilides often proceed in solution via an enolate form of the respective substrates,[7-9] such a process, resulting in **2**, cannot be invoked in an explanation of the color of the crystalline state for two reasons. First the UV spectra in chloroform solution of numerous compounds 1 exhibit absorption maxima in the range of 350–425 nm,[9] while the crystalline forms show maxima in the range of 400–700 nm.[10] This suggests that the light absorption phenomenon in solution is electronically dis-

(1) Lilly Research Laboratories, Eli Lilly and Company, Indianapolis, IN, 46285.
(2) Möhlau, R. *Ber. Dtsch. Chem. Ges.* **1882**, *15*, 2466.
(3) Chatterjee, B. G.; Abdulla, R. F. *Z. Naturforsch., Sect. B: Anorg. Chem., Org. Chem., Biochem., Biophys., Biol.* **1971**, *25B*, 181.
(4) Chatterjee, B. G.; Lahiri, S. K.; Abdulla, R. F. *Z. Naturforsch., Sect. B: Anorg. Chem., Org. Chem., Biochem., Biophys., Biol.* **1971** *25B*, 675.
(5) Abdulla, R. F.; Lahiri, S. K.; Crabb, T. A.; Cahill, R. *Z. Naturforsch., Sect. B: Anorg. Chem., Org. Chem., Biochem., Biophys., Biol.* **1971**, *26B*, 95.
(6) Abdulla, R. F.; Bannerji, A. N. *Z. Naturforsch., Sect. B: Anorg. Chem., Org. Chem., Biochem., Biophys., Biol.* **1971**, *26B*, 1140.
(7) Abdulla, R. F. *Z. Naturforsch., Sect. B: Anorg. Chem., Org. Chem., Biochem., Biophys., Biol.* **1972**, *27B*, 1465.
(8) Filacchioni, G.; Artico, M.; Brosio-E.; Conti, F. *Farmaco, Ed. Sci.* **1978**, *33*, 48.
(9) Kallmeyer, H. J.; Wagner, E. *Arch Pharm. (Weinheim, Ger.)* **1980**, *313*, 315.
(10) Smirnov, E. A.; Yakovenko, T. I. *Izv. Vyssh. Uchebn. Zaved., Khim. Khim. Tekhnol.* **1969**, *12* (10), 1375.

0022-3263/85/1950-3502$01.50/0

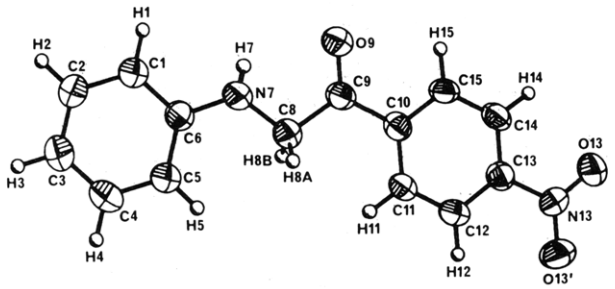

Figure 1. ORTEP plot of (*p*-nitrophenacyl)aniline (**1a**) with the numbering scheme used in the crystallographic study.

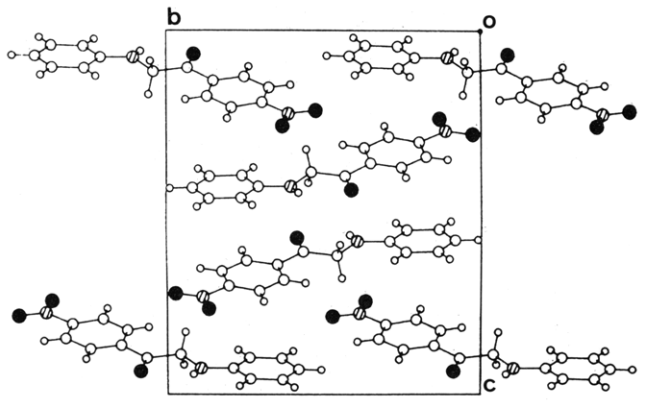

Figure 2. Crystal packing for **1a**, as viewed down the *a* axis. Small open circles are hydrogen atoms and larger open circles, carbon; cross-hatched circles are nitrogen atoms and solid circles, oxygen.

Table II. Atom Coordinates ($\times 10^4$) and Temperature Factors ($Å^2 \times 10^3$)

atom	*x*	*y*	*z*	U^a
C(1)	8846 (3)	7637 (2)	4559 (1)	54 (1)
C(2)	8793 (4)	8669 (2)	4583 (2)	60 (1)
C(3)	6909 (4)	9177 (2)	4288 (2)	68 (1)
C(4)	5093 (4)	8645 (2)	3974 (1)	61 (1)
C(5)	5120 (3)	7610 (2)	3951 (1)	53 (1)
C(6)	7009 (3)	7091 (2)	4249 (1)	48 (1)
N(7)	7109 (3)	6057 (2)	4250 (2)	72 (1)
C(8)	5473 (3)	5410 (2)	3859 (1)	51 (1)
C(9)	6189 (3)	4329 (1)	3965 (1)	48 (1)
O(9)	7942 (3)	4130 (1)	4342 (1)	67 (1)
C(10)	4695 (3)	3513 (2)	3611 (1)	45 (1)
C(11)	2664 (4)	3711 (2)	3192 (1)	49 (1)
C(12)	1291 (3)	2938 (2)	2893 (1)	51 (1)
C(13)	2023 (3)	1961 (1)	3032 (1)	46 (1)
N(13)	606 (3)	1127 (1)	2730 (1)	54 (2)
O(13)	1299 (3)	263 (1)	2817 (1)	77 (1)
O(13′)	−1208 (3)	1319 (1)	2399 (1)	88 (1)
C(14)	4046 (3)	1741 (1)	3431 (1)	49 (1)
C(15)	5400 (3)	2526 (2)	3723 (1)	48 (1)
O(13′)	−1208 (3)	1319 (1)	2399 (1)	88 (1)

[a] Equivalent isotropic *U* defined as one-third of the trace of the orthogonalized $\mathbf{U}_{ij}$ tensor.

tinct from that in the solid state. Second, there is no evidence in the literature that any of the compounds **1** exist in equilibria with enolic forms in solution or as enols in the solid state.[5-9] Indeed it appears that charge transfer[11] is more relevant to the issue of the color of compounds **1** than enolization.

In an effort to resolve the solid-state structure of the (nitrophenacyl)anilines and its impact on their color, an X-ray diffraction study of **1a** was undertaken. The results

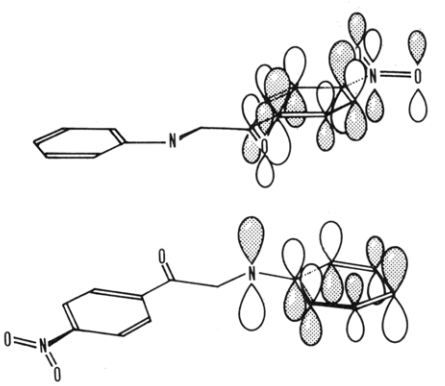

Figure 3. MNDO highest occupied molecular orbitals of $\mathbf{1a}^{-\cdot}$ (upper) and $\mathbf{1a}^{+\cdot}$ (lower), each of which is singly occupied. The size of the LCAO–MO coefficients are roughly reflected in the size of the lobes on each center.

Table III. Ionization Potentials (eV) Predicted by MO Calculations on 1a and 3

	1a	3[a]
EH	10.7	12.8
MINDO/3	7.9	9.2
MNDO	8.5	9.4

[a] Experimental value is 9.247 eV.[19]

Table IV. MNDO Predicted Heats of Formation (kcal/mol) for 1a and 3

	1a	3
ground state	48.0	21.2
radical anion	−2.4	23.4
radical cation	235.0	230.1

Table V. MNDO Net Atomic Charges (in Electron Units) for the Highly Polar Groups in 1a

	N—H		C=O		O=N=O		
ground state	−0.39	+0.20	+0.25	−0.28	−0.33	+0.48	−0.33
radical anion	−0.38	+0.20	+0.24	−0.40	−0.44	+0.48	−0.45
radical cation	−0.19	+0.24	+0.26	−0.26	−0.31	+0.48	−0.32

of this study show that **1a** (Figure 1 and Table II) is nearly planar with no atoms other than hydrogen deviating from the weighted least-squares plane by more than 0.09 Å. The crystal packing (Figure 2) shows stacks of coplanar molecules, spaced 3.54 Å apart. Adjacent *p*-nitrophenyl and aniline rings are interleaved in a continuous, alternating stack of paired molecules, strongly suggesting the existence of a charge-transfer complex in the crystal. The X-ray crystal structure study eliminates speculation on contributions to the color by enolic forms **2** or by the *intramolecular* interaction of the electron-accepting nitrobenzoyl group and the electron-donating arylamine part of the molecule, with the donor and acceptor portions of the molecule folded, one above the other, as suggested by Kallmayer and Wagner.[9]

In order to assess the likelihood of a charge-transfer band giving rise to the red color observed in crystalline *N*-(4′-nitrophenacyl)aniline, **1a**, and, by analogy, in its analogues, the nature of the frontier molecular orbitals was determined by semiempirical MO calculations. The methods employed were extended Hückel (EH),[12,13]

(11) Briegleb, G. "Elektronen Donator-Acceptor Komplexe"; Springer-Verlag: Berlin, 1961.

(12) Hoffmann, R. *J. Chem. Phys.* **1963**, *39*, 1397. Ammeter, J. H.; Bürgi, H.-B.; Thibeault, J. C.; Hoffmann, R. *J. Am. Chem. Soc.* **1978**, *100*, 3686. Boyd, D. B., presented at the Quantum Chemistry Program Exchange Workshop of Practical Aspects of Semiempirical Techniques, Bloomington, IN, June 19–22, 1983, and references cited therein.

MINDO/3,[14,15] and MNDO.[16,17] Results of the calculations on **1a** are compared to those of benzene **3**, so that a qualitative comparison of the ease of electronic excitation in these two molecules can be made.

The results of the calculations are summarized in Tables III–V. The Koopmans' theorem[18] ionization potentials from the MO methods (Table III) illustrate that it is 1–2 eV easier to remove an electron from **1a** than from **3**.[19] The EH eigenvalues likewise show a much smaller gap between the highest occupied MO (HOMO) and the lowest unoccupied MO (LUMO) in **1a** (0.96 eV) than in **3** (4.45 eV). A small gap between filled and empty EH MOs is, of course, characteristic of low excitation energy.[20]

Reported in Table IV are the predicted heats of formation of the parent molecules **1a** and **3** and the radicals formed by adding one electron or removing one electron from the molecules. These energies can be used to compute the vertical (fixed geometry) energy change for the process:

$$2M \rightarrow M^{+\cdot} + M^{-\cdot}$$

In effect, the energy for this hypothetical gas-phase process is the charge-transfer energy for two isolated molecules of a compound. The charge-transfer energy calculated this way will be overestimated because actual intermolecular electrostatic interactions are neglected. Hence the following predicted values should be viewed as upper limits. For **1a**, the energy change is 5.9 eV (equivalent to 209 nm). The energy change for **3** of 9.2 eV (135 nm) is much larger. Whereas these simply calculated energy changes cannot be compared quantitatively to the electronic spectra of crystalline **1a** and **3**, they do show that charge transfer is a relatively low-energy process in **1a**.

The nature of the MOs that are involved in the charge-transfer process is shown schematically in Figure 3. The upper orbital is the HOMO of the radical anion of **1a** as predicted by MNDO. The lower orbital is the HOMO of the radical cation of **1a**. The MNDO LUMO and HOMO of the parent molecule **1a** have shapes closely similar to these. As seen in Figure 3, the HOMO is almost entirely localized on the aniline portion of **1a**, whereas the LUMO is almost entirely localized on the *p*-nitrobenzoyl moiety. In the crystal packing diagram (Figure 2), the aniline and *p*-nitrobenzoyl rings overlap by about 50% when viewed along an axis perpendicular to the parallel molecular planes. Thus, the molecules are stacked in the crystal for strong interaction between the HOMO and LUMO of two different molecules of **1a**.

The character of the HOMO and LUMO of **1a** means that charge transfer is from the aniline ring to the *p*-nitrobenzoyl ring. That this should be the preferred direction of the charge transfer is consistent with the electronic effects of the substituents on each ring. The nitrogen atom of aniline is a donor of π-electron density. The N 2p π-electron population (1.84) is less than 2.0, and of the 0.16 electron that is donated, 0.12 electron populates the π-orbitals of the aryl ring of the aniline group. The excess π-electron density on the aryl ring of the aniline moiety raises the level of the HOMO relative to that of an unsubstituted aromatic ring and makes it easier to remove an electron.

The π-electron-withdrawing groups on the phenacyl moiety, viz., nitro and carbonyl, stabilize an extra electron added to the LUMO of **1a**. The MNDO π-electron populations are 0.74 and 1.29 for the C=O atoms and 1.05, 1.49, and 1.49 for the NO_2 atoms. Thus, each of these groups as a whole has an excess of about 0.03 π-electrons. The net deficiency of π-electrons on the phenyl ring of the *p*-nitrobenzoyl moiety is 0.04. (A complete accounting for all the π-electrons in the molecule shows that there is also a minor hyperconjugative shift of 0.02 electron away from the methylene bridge to other parts of the molecule.)

The total molecular dipole moment of **1a** is 3.1 D by MNDO and 3.2 D by MINDO/3. The direction of the dipole is along the long axis of the molecule with the aniline ring at the positive end and the nitro group at the negative end of the dipole. Taking into account both the π-and σ-electron distributions, the MNDO net atomic charges can be subtotaled to show that the aniline moiety bears a net excess of 0.15 electron, the *p*-nitrobenzoyl moiety carries an excess of 0.05 electron, and the methylene group is deficient by 0.20 electron. The molecules in the crystal lattice are stacked with their dipoles in a favorable head-to-tail alignment for each stacked pair.

The crystal packing arrangement shows no strong hydrogen bonds. There is no diminution of the electrostatic potential field around the polar groups capable of hydrogen bonding when the molecule is in a charge-transfer state as seen from the charge distributions in Table V. Thus, the charge-transfer and dispersive interactions must guide the pairwise stacked packing arrangement.

In conclusion, we feel that the crystallographic data and the quantum mechanical calculations provide a rationale for invoking intermolecular charge transfer in crystalline **1a** to explain the color of the (nitrophenacyl)anilines.

Experimental Section

Compound **1a** was prepared by procedures outlined in the literature[3,8] and was recrystallized X3 from ethyl acetate.

X-ray Diffraction Studies on 1a. Compound **1a** exists as red (scarlet) prisms in the space group $P2_1/c$, with four molecules in a unit cell having the dimensions $a = 6.130 \pm 0.001$ Å, $b = 13.301 \pm 0.003$ Å, $c = 14.992 \pm 0.004$ Å, and $\beta = 93.45 \pm 0.02°$. The calculated density, 1.395 g cm^{-3}, is somewhat high for a compound containing no atom heavier than oxygen, implying a tightly packed crystal. A total of 1886 reflections was measured on an automated four-circle diffractometer, using monochromatic copper radiation. The structure was solved by the direct methods routines of the SHELXTL program library and refined by the least-squares method to $R = 0.065$, with anisotropic temperature factors for

(13) Howell, J.; Rossi, A.; Wallace, D.; Haraki, K.; Hoffmann, R. *QCPE Catalog* **1977**, *11*, 344. The FORTICON8 program was run with default values for all options. The atomic coordinates for atoms other than hydrogen were taken from the X-ray data on **1a** and from standard bond lengths and bond angles for **3**. All hydrogen atoms were added with standard bond lengths and bond angles (Pople, J. A.; Gordon, M. *J. Am. Chem. Soc.* **1967**, *89*, 4253) because X-ray diffraction systematically underestimates C–H and N–H bond lengths. In order to get *QCPE 344* to run on a VAX 11/780, the GIVENS matrix diagonalization routine was replaced by GIVEIS (formerly NRCC program NDO3 by C. Moler and D. Spangler).

(14) Bingham, R. C.; Dewar, M. J. S.; Lo, D. H. *J. Am. Chem. Soc.* **1975**, *97*, 1285, 1294, 1302, 1307.

(15) Stewart, J. J. P. *QCPE Bulletin* **1983**, *3*, 43. The MOPAC program (*QCPE 455*) was used for the MNDO and MINDO/3 calculations. The default options were used, except that the Pulay self-consistent convergence procedure had to be used for the non-ground-state calculations on benzene. The structure of **1a** and **3** were optimized while constraining the molecules to be planar in order to save computer time. Starting geometrical data came from standard bond lengths and bond angles from the X-ray data on **1a**. Calculations on the radical anion and cation of **1a** and **3** were done while holding the geometric parameters fixed at the optimized values for the ground state structures. (The structure of **1a** was too large to attempt an MNDO supermolecule calculation on a paired set of molecules.)

(16) Dewar, M. J. S.; Thiel, W. *J. Am. Chem. Soc.* **1977**, *99*, 4899, 4907.

(17) Boyd, D. B. *Drug Inf. J.* **1983**, *17*, 121.

(18) Koopmans, T. *Physica (Amsterdam)* **1933**, *1*, 104. See also footnote 41 in: Boyd, D. B.; Riehl, J. P.; Richardson, F. S. *Tetrahedron* **1979**, *35*, 1499.

(19) Herzberg, G. "Molecular Spectra and Molecular Structure. III. Electronic Spectra and Electronic Structure of Polyatomic Molecules"; D. Van Nostrand: Princeton, New Jersey, 1967; p 664.

(20) Boyd, D. B. *J. Am. Chem. Soc.* **1972**, *94*, 6513, 8799.

all atoms except hydrogen. Hydrogen atoms were included with isotropic temperature factors at calculated positions.

Acknowledgment. The FORTICON8 and MOPAC computer programs were made available by R. Hoffmann and J. J. P. Stewart, respectively, through the Quantum Chemistry Program Exchange, Indiana University, Bloomington, IN. GIVEIS was kindly furnished by S. Hagstrom, QCPE, Indiana University, Bloomington, IN.

Supplementary Material Available: Tables VI–IX, bond lengths, bond angles, anisotropic temperature factors, and hydrogen atom coordinates, respectively (3 pages). Ordering information is given on any current masthead page.

Disaccharide-Derived 2-Oxo- and 2-Oximinoglycosyl Bromides: Novel, Conveniently Accessible Building Blocks for the Expedient Construction of Oligosaccharides with α-D-Glucosamine, β-D-Mannose, and β-D-Mannosamine as Constituent Sugars[1]

Frieder W. Lichtenthaler,* Eisuke Kaji, and Sabine Weprek

Institut für Organische Chemie der Technischen Hochschule Darmstadt, D-6100 Darmstadt, West Germany

Received November 21, 1984

A concise, practical, large-scale adaptable approach has been developed for the transformation of bulk disaccharides such as lactose, maltose, and cellobiose into disaccharide building blocks suitably functionalized for direct glycobiosylation, i.e., benzoylated *glycosyl-(1→4)-glycosulosyl bromides* (**7**, **20**) and *glycosyl-(1→4)-2-benzooximinoglycosyl bromides* (**8**, **15**, **21**, and **22**). The methodology elaborated starts with the conversion of the basic disaccharides by benzoylation, HBr treatment, and dehydrobromination into their 2-hydroxyglycal esters **6**, **17a**, and **17b**; it is followed either by NBS-promoted methanolysis that effectively (85–90%) delivers the hexa-*O*-benzoyl-α-D-glycobiosulosyl bromides **7** and **20**, or, alternatively, by the high-yielding (70–75%) three-step sequence hydroxylaminolysis → benzoylation → photobromination, which provides the lactose-, maltose-, and cellobiose-derived heptabenzoyl-α-D-oximinoglycosyl bromides **8**, **21**, and **22**. The broad utility of these novel disaccharide building blocks with a nonparticipating group next to the anomeric center resides in the ease and uniformity with which stereocontrol over glycosidations can be effected: silver carbonate induced alcoholyses with simple primary and secondary hydroxyl components exclusively provide the β-glycosidulose **29** or its oximes (**24–26**), while the same reaction promoted with *s*-collidine in dioxane delivers the α-oximino glycosides **32–35** with high α-selectivity. In the disaccharides thus obtained reduction of the 2-oxo ($NaBH_4$) and 2-benzoyloximino functions (BH_3/THF) proceed with complete stereoanomeric control, hydride addition from the side opposite to the anomeric substituent converting α-anomers into α-D-glucosamine-containing disaccharides, e.g., α-D-lactosaminides **36–38**, while β-anomers as cleanly elaborate products with β-D-mannose (**30**) and β-D-mannosamine residues (**27**, **28**). Thus, the disaccharide building blocks newly introduced here not only provide an effective means for the attachment of α-linked lactosamine, maltosamine, and cellobiosamine units onto a given sugar hydroxyl but, moreover, are particularly serviceable for the methodologically more unique annelation of glycosyl-(1→4)-β-D-mannose and glycosyl-(1→4)-β-D-mannosamine blocks.

Oligosaccharides composed of more than one type of sugar unit such as the human blood group determinantes and the bacterial antigens are major carriers of biological information[2] which necessitates their regio- and stereocontrolled synthesis on a preparative scale. The impressive advances made toward this end within the past decade[3] usually comprised the stepwise construction of oligosaccharides from suitably blocked, anomerically activated monosaccharide components resulting in elongation of the saccharide chain by one sugar unit; alternately, if a disaccharide derivative was used for extension, it was synthesized a priori from the respective monosaccharide components.[3]

Considerably less attention has been given to approaches that explicitly utilize the synthetic potential inherent in the common, readily accessible disaccharides, when suitably protected and anomerically activated lactose, maltose, and cellobiose, for example, represent disaccharide building blocks with useful glycobiosylation capacity. First examples of monosaccharide glycobiosylations with simple peracylated disaccharide halogenoses date back to the thirties[4–6]—with moderate yields and questionable anom-

Scheme I

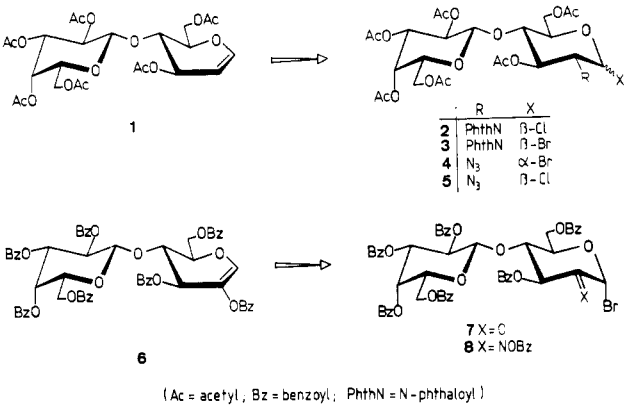

(1) This paper is dedicated to Professor R. U. Lemieux in appreciation of his pioneering contributions to carbohydrate chemistry in general and to the synthesis of oligosaccharides in particular, on the occasion of his 65th birthday.

(2) Montreuil, J. *Adv. Carbohydr. Chem. Biochem.* **1980**, *37*, 157. Jennings, H. J. *Ibid.* **1983**, *41*, 155.

(3) For pertinent accounts of this development, see: Lemieux, R. U. *Chem. Soc. Rev.* **1978**, *7*, 423. Bochkov, A. F.; Zaikov, G. E. "Chemistry of the *O*-Glycosidic Bond: Formation and Cleavage"; Pergamon: Oxford, 1979; pp 80–153. Paulsen, H. *Angew. Chem., Int. Ed. Engl.* **1982**, *21*, 155. Nashed, M. A.; Anderson, L. A. *J. Am. Chem. Soc.* **1982**, *104*, 7282.

(4) Helferich, B.; Schäfer, W. *Liebigs Ann. Chem.* **1926**, *450*, 229. Helferich, B.; Bredereck, H. *Ibid.* **1928**, *465*, 166.

0022-3263/85/1950-3505$01.50/0